

Light-induced electron spin resonance in amorphous hydrogenated germanium

F. C. Marques,^{a)} M. M. de Lima, Jr.,^{b)} and P. C. Taylor

Department of Physics, University of Utah, Salt Lake City, Utah 84112

(Received 7 April 1999; accepted for publication 27 April 1999)

We report the observation of light-induced electron spin resonance (LESR) in amorphous hydrogenated germanium. Two new lines with zero crossings near $g=2.01$ and $g=2.03$ were detected and ascribed to electrons and holes in the conduction- and valence-band-tail states, respectively. The ratio between the LESR spin densities of both lines is approximately one, suggesting the absence of spin pairing, charge defect creation, or LESR of dangling bonds. The growth and decay spectra exhibit dispersive behavior with a dispersion parameter ~ 0.5 . The decay spectrum is best fit assuming bimolecular recombination. The LESR spin density depends weakly on the photogeneration rate as a sublinear power law. © 1999 American Institute of Physics. [S0003-6951(99)03925-X]

Paramagnetic centers in amorphous silicon and germanium thin films were first identified by Brodsky and Title in 1969 by electron spin resonance (ESR) measurements.¹ The strength of the ESR signal is proportional to the number of paramagnetic centers, providing a powerful tool to probe the microstructure of these materials. The dominant ESR centers in hydrogenated amorphous silicon (*a*-Si:H) and hydrogenated amorphous germanium (*a*-Ge:H) are attributed, respectively, to unpaired electrons at neutral silicon or germanium dangling bonds in the bulk of the films. Two additional paramagnetic centers have also been identified in phosphorous- and boron-doped *a*-Si:H,^{2,3} and *a*-Ge:H,⁴ and ascribed to localized electrons and holes in the conduction- and valence-band tails, respectively. Similar lines have been detected in *a*-Si:H by light-induced electron spin resonance (LESR).^{2,3} In spite of a number of attempts over the last 20 years,^{5,6} no similar LESR has been detected in *a*-Ge:H. In this letter we present the observation of LESR in *a*-Ge:H, and attribute the signals to holes and electrons trapped in the valence- and conduction-band tails, respectively. The observation of LESR in *a*-Ge:H allows the recombination kinetics and doping mechanisms in this amorphous semiconductor to be compared with those observed in *a*-Si:H and therefore allows potentially universal features to be identified.

The *a*-Ge:H films were deposited by radio frequency (rf) sputtering using the conditions described elsewhere.⁷ A film deposited onto aluminum foil was removed from the substrate by etching the aluminum with dilute HCl. The resultant powdered film was placed in an ESR quartz tube. A Bruker-200D-SRC spectrometer operating at X band (~ 9.52 GHz) was used. The measurements were taken by sweeping the magnetic field while the sample was illuminated using a Nd-yttrium-aluminum-garnet YAG laser ($h\nu=1.17$ eV).

Before irradiation, the density of neutral germanium dangling bonds was $\sim 2 \times 10^{17} \text{ cm}^{-3}$ as measured by ESR. Films deposited under similar conditions have ~ 15 at. % total hydrogen concentration as obtained from elastic recoil detection analysis (ERDA) optical band gaps of $E_{04} \sim 1.2$ eV and $E_{\text{tauc}} \sim 1.1$ eV, Urbach energy of ~ 60 meV from photothermal deflection spectroscopy, and activation energy for electrical conductivity of ~ 0.5 eV. These values are among the best data reported in the literature for *a*-Ge:H films.

The LESR derivative spectrum, as shown in Fig. 1(a), resembles those obtained for *a*-Si:H³ and is apparently also composed of two components, one narrow and one broad. In *a*-Si:H the narrow line, which peaks at a higher field, has been attributed to electrons trapped in conduction-band-tail states, while the broad line has been ascribed to holes in valence-band-tail states. The LESR spectrum of Fig. 1(a) was fit assuming two paramagnetic sites. Because of limited information, the LESR powder-pattern line shapes were calculated assuming the same anisotropy in the g tensor as that which fits the dark ESR response due to Ge dangling bonds. The width introduced by the anisotropy is consistent with that expected by scaling the upper bounds for the anisotropy in the dark ESR and LESR observed in *a*-Si:H by the ratios of the spin-orbit coupling constants for Si and Ge ($\lambda_{\text{Ge}}=0.138$ eV and $\lambda_{\text{Si}}=0.019$ eV).⁸ This procedure amounts to assuming that the dangling bond, the electron trapped in a conduction-band-tail state, and the hole trapped in a valence-band-tail state are electronically similar for *a*-Si:H and *a*-Ge:H. The two new LESR lines observed in *a*-Ge:H after light excitation are: (1) a broad resonance with a peak-to-peak width of ~ 60 G centered near $g=2.03$ and (2) a narrow resonance with a width ~ 26 G centered at $g=2.01$. The two LESR lines saturate at different microwave power levels, which is an indication that they are due to two different ESR centers. In particular, the narrow line saturates at a higher microwave power, which is different from the behavior observed previously in *a*-Si:H.⁹

ESR experiments in phosphorous- and boron-doped *a*-Ge:H exhibit two lines, $g=2.012$ (width=33 G) and $g=2.0535$ (width=112 G), which have been attributed to

^{a)}Permanent address: Universidade Estadual de Campinas, Unicamp, Instituto de Física "Gleb Wataghin" 13083-970, Campinas—SP, Brasil. Electronic mail: marques@ifi.unicamp.br

^{b)}Present address: Universidade Estadual de Campinas, Unicamp, Instituto de Física "Gleb Wataghin" 13083-970, Campinas—SP, Brasil. Electronic mail: mmlimajr@ifi.unicamp.br

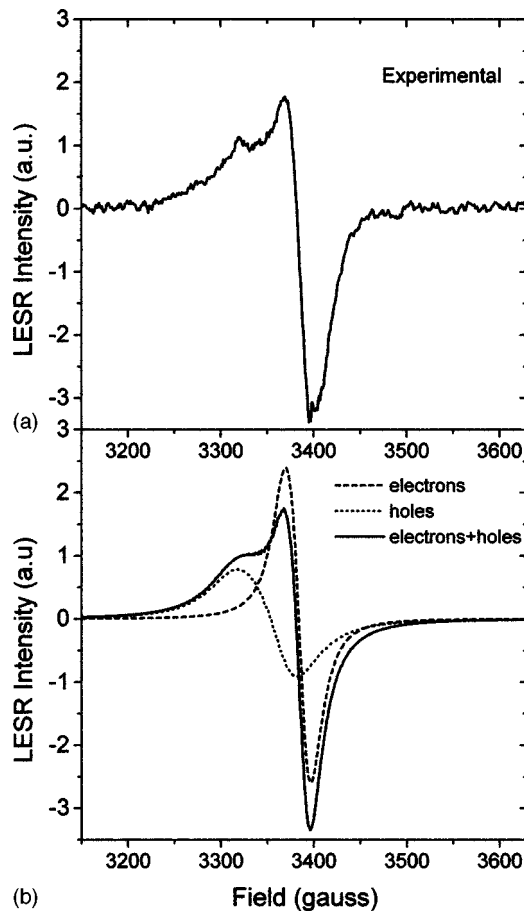


FIG. 1. (a) LESR of *a*-Ge:H, obtained by subtracting the signal in the dark from that under light excitation. (b) Fit to the experimental spectrum using two ESR centers.

electrons and holes in the conduction- and valence-band tails for *n*-type and *p*-type films, respectively.⁴ The features of the narrow and broad lines of the spectrum of Fig. 1 are similar, although certainly not identical, to those obtained by ESR in *n*-type and *p*-type *a*-Ge:H. In *a*-Si:H it has also been observed that the LESR features of both electrons and holes and the ESR of *n*-type and *p*-type films, respectively, are not identical. In particular, the ESR line shapes in the doped samples depend on the doping level. Because of these similarities and the resemblance with the LESR of *a*-Si:H we attribute the narrow and the broad lines observed in the LESR of *a*-Ge:H to electrons and holes trapped in the conduction- and valence-band tails, respectively.

From the results of the computer simulation we find that the ratio between the density of paramagnetic spins due to holes and electrons, C_p/C_n , is about 1 ± 0.3 . In *a*-Si:H this ratio depends on a number of conditions and is typically in the range 2–5.^{9,10} The origin of the deviation from a one-to-one ratio between the lines attributed to holes and electrons in *a*-Si:H has been a matter of some debate. This deviation has been attributed to spin pairing, to a change in the ratio of charged to neutral defect densities,¹⁰ or to certain artifacts of the ESR measurement technique.⁹ In *a*-Ge:H it appears that none of these mechanisms is important. Due to the high density of dangling bonds in the *a*-Ge:H ($\sim 2 \times 10^{17} \text{ cm}^{-3}$ in the sample used in this study) compared to the density of the optically excited electrons and holes ($\sim 2 \times 10^{16} \text{ cm}^{-3}$), a

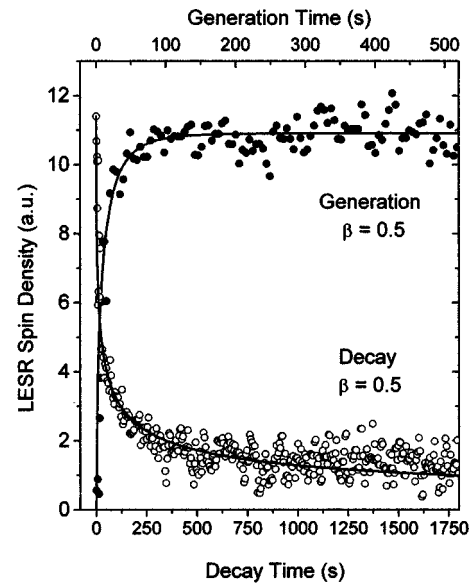


FIG. 2. Generation and decay of the LESR signal at 3400 G. At this magnetic field the signal is attributed mainly to electrons trapped in conduction-band tail. The data are averaged over four independent measurements, each performed without previous exposure to light.

small positive (or negative) LESR of the dangling bonds would cause a dramatic change in the hole-to-electron ratio. In *a*-Si:H the ratio between the LESR and dark ESR due to silicon dangling bonds is usually much greater than unity. Since C_p/C_n is near unity one can conclude that spin pairing and changes in the densities of neutral or charged defects are not important for the interpretation of the LESR in *a*-Ge:H. These results may prove useful for understanding the origin of the deviation in *a*-Si:H.

Information concerning the kinetics of the photogenerated carriers can be obtained through an analysis of the time dependence of the LESR. In Fig. 2 we show generation and decay curves of the LESR centered at 3400 G in *a*-Ge:H. At this magnetic field the LESR is mainly attributed to electrons in the conduction-band tail. As also occurs in *a*-Si:H, some photogenerated carriers are still present about 30 min after the light is turned off. The generation and decay of the broad line (measured at a fixed field of 3300 G, and attributed to holes), follow the same time dependencies as the generation and decay of the narrow line. A ratio of ~ 1 was obtained between both lines as a function of time. The solid curves in Fig. 2 are fits assuming a dispersive model for deeply trapped carriers. See Refs. 9 and 11 for the details of the kinetic model, which was developed for *a*-Si:H. In this model the recombination is assumed to be bimolecular. In *a*-Ge:H a dispersive parameter $\beta \sim 0.5$ was found for both generation and decay. Similar results were obtained for *a*-Si:H.⁹

Using neutral density filters we measured the LESR signal intensity, N , as a function of light intensity, I , at a fixed field of 3400 G. As shown in Fig. 3 the signal increases weakly with light intensity. For intermediate generation rates $N \propto I^\gamma$, where $\gamma \sim 0.27$. This behavior is also similar to that reported for *a*-Si:H.^{3,9,11,12} Recently, a model due to Levin, Marianer, and Shklevskii¹³ has predicted a weak power law dependence, $\gamma \sim 0.16$, due to bimolecular recombination of the photogenerated carriers in amorphous semiconductors.

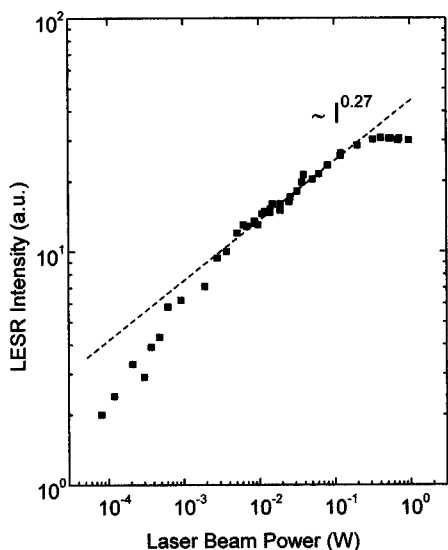


FIG. 3. Intensity of the LESR as a function of the ND:YAG laser power. The dotted line is a fit to the intermediate power range. At 1 W laser power, the intensity at the sample is approximately 10 W/cm².

This model considers the probability functions for both geminate and distant-pairs recombination processes as a function of time and light intensity. Our results for *a*-Ge:H support this model in which nongeminate (distant-pair) recombination dominates over all experimentally accessible excitation intensities. For laser powers greater than about 0.1 W, the signal starts to saturate, probably due to heating of the sample. At low laser powers one does not reach equilibrium (saturation of the signal level as a function of time) of the LESR on the time scale employed (5–10 min) because of very small generation rates.¹¹

There are several reasons why LESR had not been observed in *a*-Ge:H after more than two decades of investigation. The main reason is the fairly large number of germanium dangling bonds, which normally lies in the 10¹⁸–10²⁰ cm⁻³ range, and masks the observation of any LESR. For instance, even for the relatively high quality *a*-Ge:H studied here, with $\sim 2 \times 10^{17}$ cm⁻³ dangling bonds, the density of photo-excited carriers is about one order of magnitude smaller, $\sim 2 \times 10^{16}$ cm⁻³. Second, the line width W is very large, due to the large spin-orbit coupling constant of germanium. Since the intensity of the derivative signal goes approximately as W^{-2} , the signal is strongly reduced.

For example, the measured peak intensity of the electron derivative line in *a*-Ge:H is roughly reduced to $(W_{\text{Ge}}/W_{\text{Si}})^{-2} \sim 10\%$ of that of *a*-Si:H, for the same number of excited spins. Third, the LESR signal depends only weakly on the light intensity, $N \propto I^{0.27}$. In Fig. 3 the power was varied by more than four orders of magnitude, while the LESR intensity varied only by about one order of magnitude. Thus, using high power is not of much help for measuring LESR in *a*-Ge:H. Fourth, the absorption coefficient of *a*-Ge:H at ~ 2.0 eV, where most previous experiments were performed, is roughly one order of magnitude higher than the absorption coefficient near the band gap ($E_{04} \sim 1.2$ eV, $E_{\text{tauc}} \sim 1.1$ eV). The use of photon energies near the band gap allows the excitation of carriers throughout the bulk of the film. This condition was achieved using a Nd:YAG laser (1.17 eV).

In summary, two paramagnetic centers are found in *a*-Ge:H after light excitation. These two centers are attributed to unpaired electrons and holes in the conduction- and valence-band tails, respectively. The generation and decay curves are characterized by dispersive behavior with a dispersive parameter, β , approximately 0.5. The decay is bimolecular, and the LESR depends only weakly on light intensity, $N \propto I^{0.27}$. These results are very similar to those obtained for *a*-Si:H.

The authors are in debt to Prof. F. L. Freire for ERDA measurements and to CNPq and FAPESP for partial support. This work was also supported by NREL under Subcontract No. XAK-8-17619-13.

¹M. H. Brodsky and R. S. Title, Phys. Rev. Lett. **23**, 581 (1969).

²J. C. Knights, D. K. Biegelsen, and I. Solomon, Solid State Commun. **22**, 133 (1977).

³R. A. Street and D. K. Biegelsen, Solid State Commun. **33**, 1159 (1980).

⁴M. Stutzmann and J. Stuke, Solid State Commun. **47**, 635 (1983).

⁵J. R. Pawlik and W. Paul, Proceedings of the 7th International Conference on Amorphous and Liquid Semiconductors (1977), p. 437.

⁶M. H. Brodsky, *Amorphous Semiconductors* (Springer, Berlin, 1985).

⁷F. C. Marques and I. Chambouleyron, Proceedings of the 9th European Photovoltaic Solar Energy Conference (1989), p. 1042.

⁸G. E. Moore, Natl. Bur. Stand., Cir. No. 467 (1949).

⁹B. Yan and P. C. Taylor, Mater. Res. Soc. Symp. Proc. **507**, 787 (1998).

¹⁰G. Schumm, W. B. Jackson, and R. A. Street, Phys. Rev. B **48**, 14198 (1993).

¹¹B. Yan, N. Schulz, A. L. Efros, and P. C. Taylor (unpublished).

¹²F. Boulitrop and D. J. Dunstan, Solid State Commun. **44**, 841 (1982).

¹³E. I. Levin, S. Marianer, and B. I. Shklovskii, Phys. Rev. B **45**, 5906 (1992).